1995A&A...298..917K

Astron. Astrophys. 298, 917–922 (1995)

ASTRONOMY AND ASTROPHYSICS

Observations of Fe I lines in the quiet solar photosphere

A. Kučera[1,2], **J. Rybák**[1], **and H. Wöhl**[2]

[1] Astronomical Institute, Slovak Academy of Sciences, SK-05960 Tatranská Lomnica, Slovakia
[2] Kiepenheuer-Institut für Sonnenphysik, Schöneckstr. 6, D-79104 Freiburg, Germany

Received 4 March 1994 / Accepted 3 December 1994

Abstract. We investigate three sets of spectra with high spatial and spectral resolution. Each set consists of four spectra taken simultaneously with the Vacuum Tower Telescope at Izaña, Tenerife. The main spectral characteristics (continuum intensity I_c; full width at half maximum $FWHM$; residual intensity I_o) were computed for 5 magnetic and non-magnetic Fe I lines (5434.543 Å, 5576.099 Å, 6301.497 Å, 6302.499 Å, 6494.994 Å). Our results allow a diagnosis of the solar atmosphere in the vertical (two main levels of line formation) and horizontal directions (71 arcseconds). The spectra cover both interior parts of supergranular cells (purely quiet regions, PQR) and cell boundaries (moderate active regions, MAR).

The main results are: (1) We find a different continuum intensity distribution for PQRs and MARs, which reflects the existence of different patterns in these regions. The difference is also evident in the rms residual intensity fluctuation. (2) A significant minimum of the residual intensity fluctuations $(\delta I_o/\bar{I}_c)_{rms}$ occurs at a height of about 300 km. (3) At all heights of the PQRs the line widths $FWHM$ in the intergranular lanes are *larger* than the mean line width; those in the granules are *smaller*. This variation of the $FWHM$ is influenced by a magnetic effect near the centres of the intergranular lanes (reduced $FWHM$), and by the effect of convection in granules (enhanced $FWHM$). (4) The correlation $< I_c, I_o >$ reverses its sign at a height of about 250 km. The anticorrelation in the range 300 – 500 km indicates a non-convective structure, different from the photospheric granular pattern found earlier.

Key words: sun: photosphere – sun: granulation – line: profiles

1. Introduction

The granular flow seen at the Sun's surface, and the overshoot of this flow into the stably stratified layers of the solar atmosphere, is most profitably investigated by spectroscopic means. Wiehr & Kneer (1988), Holweger & Kneer (1989) and Lites et al. (1989) found differences in the spectral line profiles obtained in granules and in intergranular lanes, respectively. Nesis et al. (1992b) found an enhanced line broadening in the intergranular space and interpreted this as a manifestation of enhanced turbulence. Nesis et al. (1992a, 1993) and Hanslmeier et al. (1993) have obtained a series of spectrograms, which begin to allow a detailed analysis of the physics of individual granules and intergranular lanes. Numerical simulations (Nesis et al. 1992c) indicate that the broadening of magnetically non-sensitive lines is associated with post-shock turbulence at the boundaries of granules. General characteristics of the solar granulation are described by Dravins (1982), Muller (1985, 1989), and Spruit et al. (1990).

The aim of the present paper is to investigate whether the physical processes characterizing granules and intergranular lanes are the same at higher levels of the photosphere, or whether physical and structural changes take place. The observational basis for this paper is a series of spectrograms with high spatial and spectral resolution, taken simultaneously in four different spectral regions. The spectral lines were selected for the sake of their different magnetic sensitivity, and to cover a height range in the solar atmosphere where fluctuation and correlation data of the main spectral characteristics were not yet available. We investigate continuum characteristics, rms fluctuations of the intensity in several spectral lines, the line broadening, and correlations between these line parameters. These results will be compared with data published previously and used to obtain new insight into the physics of the solar photosphere.

2. Observations and reductions

The observations were carried out with the Vacuum Tower Telescope at the Observatorio del Teide, Tenerife, on June 21, 1992. The Echelle spectrograph was used to take spectra in four spectral regions. The telescope and the spectrograph were described by Schröter et al. (1985) and Soltau (1989). The main characteristics of the 5 observed spectral lines are presented in Table 1. All four spectral regions were recorded strictly simultaneously and with the same exposure time of 0.3 s on four CCD cameras with 1024 x 1024 pixels, in the 2 x 2 binning mode. The entrance slit was 60 μm wide, i.e. 0.28 arcseconds on the solar disk. One spatial step corresponds to 0.17 arcseconds. The dispersion of the spectra is 0.087 – 0.107 Å/mm.

© European Southern Observatory • Provided by the NASA Astrophysics Data System

1995A&A...298..917K

Table 1. Main characteristics of the observed Fe I lines.

N	LAMBDA [Å]	EQ.WIDTH [mÅ]	MULTIPLET	EX.POTEN. [eV]	LANDE FACT. g_{eff}	HEIGHT OF FORMATION [km]
(I)	5434.543	184	15	1.01	0.000	560/540*) [1]
(II)	6494.994	165	168	2.40	1.025	500/ — [2]
(III)	6301.508	127	816	3.64	1.667	340/290 [1]
(IV)	5576.099	113	686	3.43	0.000	310/270 [1]
(V)	6302.499	83	816	3.69	2.500	250/230 [1]

[1] Bruls et al. (1991); [2] Guenther & Mattig (1991); *) LTE/NLTE calculation

We used Ca^+ slit-jaw images in order to select quiet solar regions at the disk center ($\mu > 0.95$). Since the slit covered 71 arcseconds, it was not possible to completely avoid any activity of the Ca^+ network. It was therefore decided to split each spectrum into two parts: The parts without network activity are called "purely quiet regions" (PQR), while the regions with network activity are called "moderate active regions" (MAR). Both parts have a length of 31 arcseconds (the gap of 10 arcseconds in between was not used). Nevertheless some of the characteristics were estimated for the whole length of the spectrum for comparison with previous data. The whole spectrum is called "nonactive region" (NAR).

A standard reduction of the CCD images (dark current, flat field, intensity trends) was performed with the help of IDL and Kiepenheuer Institute Library procedures. These procedures, and Fast Fourier Transform techniques, were also used in order to determine the spectral line characteristics I_o, I_c, and $FWHM$. For all line characteristics we strictly used a nearby local continuum for every scan as an intensity reference. Since the CCD images cover less than 1 Å of the spectrum in each wing of a line, it was necessary to calibrate the true line continuum. This was done with the help of the Liège atlas (Delbouille et al. 1973).

Since the investigation deals with strong lines and only with relative changes of line parameters, no corrections for the influence of the spectrograph's instrumental profile and scattered light were made. These effects are considered as of secondary importance.

For the statistics of the $FWHM$ data a new procedure was used: At first mean values of $FWHM$ at "granular" and "intergranular" positions along the slit were computed, in a way similar to that of Guenther & Mattig (1991). These authors considered all profiles with a continuum intensity of 104% [I_{mean}] or higher as granular profiles, while all profiles with a continuum intensity of less than 96% were ascribed to the intergranular lanes. Thus they set a fixed threshold of ±4%. We have used a "floating" threshold in the range 90% – 110% of the mean continuum intensity, with a step width of 0.1%. This means that for the granular case we have gradually computed a mean $FWHM$ over all profiles whose continuum intensities exceeded 90.0%, 90.1%, ... 110.0%. For the intergranular lanes we have computed the mean $FWHM$ over all profiles having continuum intensities lower then 110.0%, 109.9%, ... 90.0%. To avoid contributions from some extreme isolated peaks profiles from 3 or more different positions on the slit were used. Apart from that, calculations were made only for the cases in which 10 or more profiles had intensities above (resp. below) the predefined limit of the continuum intensity.

3. Results and discussion

3.1. Continuum intensity I_c

The continuum intensities vary within the interval of 0.90 – 1.10 of the mean continuum. For the PQRs the distribution of the continuum intensity has its center of gravity shifted to 1.02. There is no such shift of the center of gravity in the histogram of MARs. These results differ from those of Hanslmeier et al. (1991); the reason may be the different quality of the spectra and the sensitivity of the results on the selection of the investigated regions.

3.2. Residual line intensity I_o

Table 2 shows rms fluctuations of the line-centre intensity I_o, averaged over all three spectra, separately for NARs, PQRs and MARs. For each line we have calculated the fluctuations of I_o relative to the mean line-core intensity $\bar{I}_o$ and relative to the mean continuum intensity $\bar{I}_c$. In Fig. 1 we show these results in dependence on the height of line formation, for which the LTE values listed in Table 2 were used. In addition we show the results of previous work (Canfield & Mehltretter 1973; Keil & Canfield 1978; Hanslmeier et al. 1990).

In the upper panel of Fig. 1 we see a general trend of *increasing* rms fluctuations of the line-core data divided by the mean line-core intensities, ranging from 5 to 15 % for a height range from 0 to 600 km. In the lower panel this trend is opposite: for the same height range of line formation we find *decreasing* rms fluctuations of the line core data divided by the mean continuum intensities, ranging from 5 to 2 %. Our data fill a gap within the range 200 to 500 km, where up to now only a few data were available. Our results represent the main trend; in addition they

© European Southern Observatory • Provided by the NASA Astrophysics Data System

1995A&A...298..917K

Table 2. Rms residual line intensity fluctuations (in %), averaged over all three spectra.

Line	Height	NARs		PQRs		MARs	
	[km]	$(\delta I_o/\bar{I}_o)_{rms}$	$(\delta I_o/\bar{I}_c)_{rms}$	$(\delta I_o/\bar{I}_o)_{rms}$	$(\delta I_o/\bar{I}_c)_{rms}$	$(\delta I_o/\bar{I}_o)_{rms}$	$(\delta I_o/\bar{I}_c)_{rms}$
I	560	14.56±0.25	2.36±0.04	13.52±0.95	2.20±0.39	15.39±1.48	2.57±0.33
II	500	10.60±0.46	2.78±0.09	9.30±0.96	2.40±0.59	11.38±1.91	2.97±0.78
III	340	9.17±1.24	2.66±0.51	5.91±1.29	1.55±0.08	10.84±2.18	3.20±1.09
IV	310	9.67±0.70	2.24±0.27	6.42±0.29	1.40±0.18	11.63±1.50	2.74±0.57
V	250	9.40±1.93	3.51±0.99	5.22±1.02	1.81±0.24	11.73±3.31	4.43±1.83

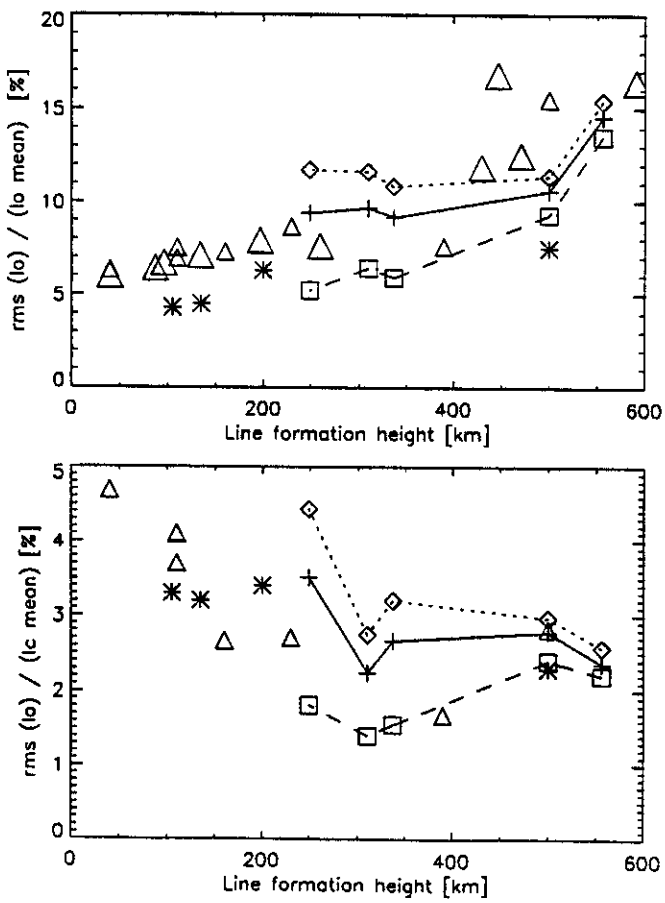

Fig. 1. Dependence of rms residual line intensity fluctuations on the height of line formation: + - averaged values over all three NARs; ◇ - averaged values over all three MARs; □ - averaged values over all three PQRs. The remaining symbols indicate data of Keil & Canfield (1978, big △), Hanslmeier et al. (1990, ∗), and Canfield & Mehltretter (1973, small △)

show the range of fluctuations between the data from the MARs, with rms fluctuations larger than from the NARs, and the data from the PQRs, with lower fluctuations. The PQR results show a minimum of 1.4 % in the rms fluctuations at about 300 km, and an increase to about 2 % at 500 km. The trends and differences seen in Fig. 1 are real: only a small fraction of the data spread is caused by the different quality of the observations and by the use of slightly different height scales by the different authors.

Intensity fluctuations in the line cores reflect mostly temperature fluctuations at the corresponding heights in the photosphere. Kneer et al. (1980) investigated the temperature fluctuations at various heights using the wings of the Mg b_2 line. Only for layers up to ~50 km, which are directly coupled to convection, they found a decrease of the fluctuations. They suggested different models of temperature fluctuations for the two different columns in the photosphere. Durrant & Nesis (1981) even found three distinct intensity (temperature) fluctuation components, coupled with convection, gravity waves and the network. Komm et al. (1990) have found two types of structure in the photosphere. Their small structures of ~1.3 arcseconds in diameter remain coherent up to higher photospheric layers (170 km), while the larger structures tend to disappear with height (Fig. 7 of their paper). They have not clarified what kind of structure dominates in the higher non-convective photosphere. Our results bear information about temperature fluctuations at heights of 300 – 500 km. A further discussion, in connection with the results of correlation calculations, will be given in Sect. 3.4.

3.3. Line width FWHM

Results of $FWHM$ computations for all 5 lines obtained by our new method are shown in Fig. 2 for the best PQR as an example. The left three panels of Fig. 2 stand for magnetic lines, the two right panels for non-magnetic lines. It is evident that at the beginning of each calculation a mean $FWHM$ is computed over all profiles, because the continua of all profiles are above the first limit continuum (0.90) for a granular case, and below the first limit continuum (1.10) for an intergranular case. Thus we obtained the "total mean $FWHM$", the dashed lines in Fig. 2. At some value of the limit continuum a departure of the mean $FWHM$ from the "total mean $FWHM$" appeared. In the upper-right panel for line I one can see a departure of the mean $FWHM$ at about 0.93 for the granules (plus signs) and at about 1.07 for the intergranular lanes (squares). For the granular case the mean $FWHM$ values *decrease* with increasing continuum limit and reach the minimum value at about 1.04 (centres of granules). In the intergranular case the mean $FWHM$ values *increase* with decreasing continuum limit, and the maximum is at 0.95 (pure intergranular lanes). These statistical results are in agreement with the results of Nesis et al. (1993) who made a direct analysis of the coupling between I_c and $FWHM$.

For further numerical comparison our detailed results for all PQRs, including the errors, are given in Table 3 for both the

© European Southern Observatory • Provided by the NASA Astrophysics Data System

1995A&A...298..917K

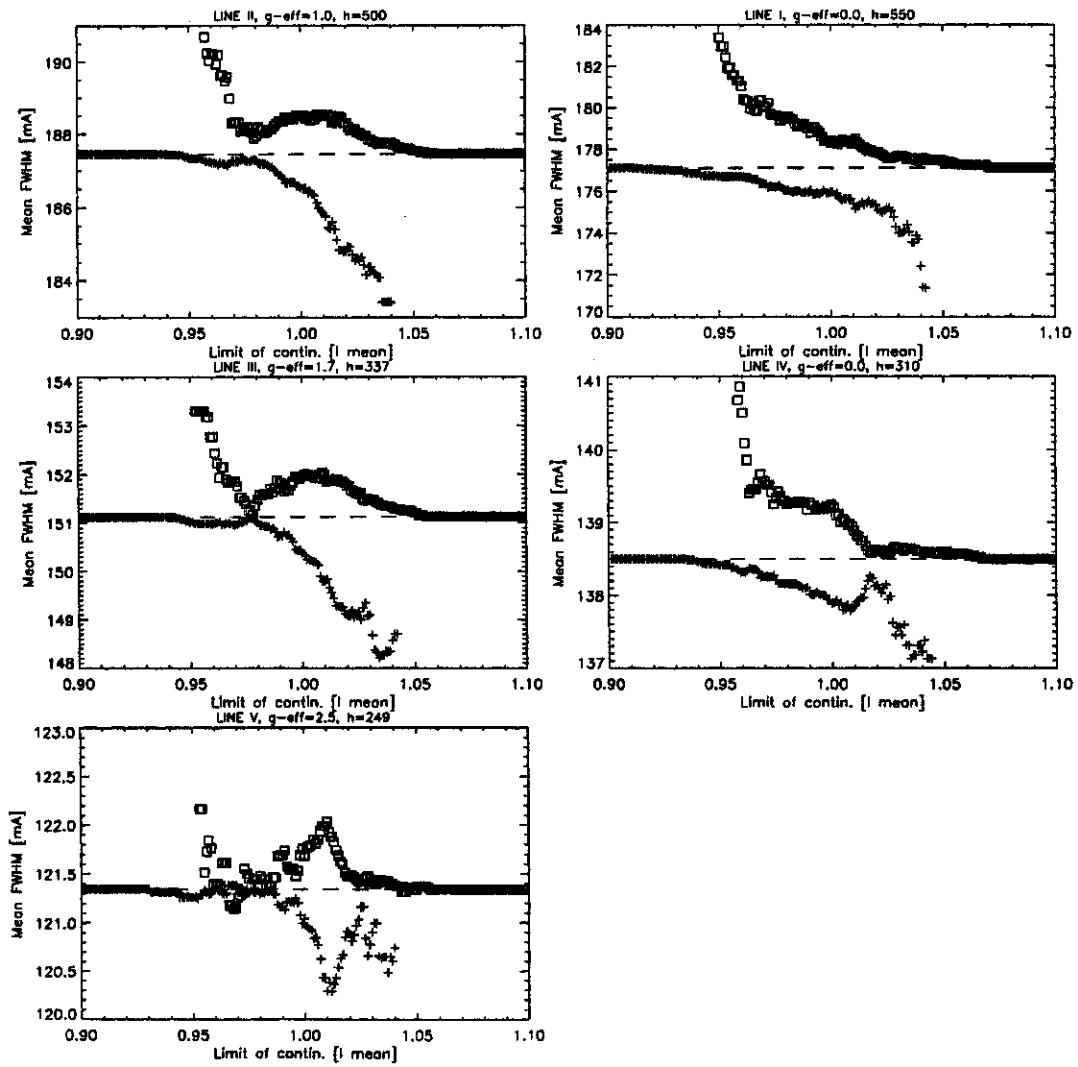

Fig. 2. Mean $FWHM$ for all 5 lines in one PQR: + - granular case, □ - intergranular case. For more information see main text (Sect. 3.3.)

4% and the floating threshold. We have found an increase of the difference of the mean $FWHM$ values for granules and intergranular lanes (Δ_{FWHM}) with height in the photosphere (last column in Table 3). The difference Δ_{FWHM} is very small for the deepest line. From the data of Nesis et al. (1991, their Fig. 2, right column) it is possible to find negative slopes which serve as an approximation of the $FWHM$ dependence on I_c for the lower photospheric layers. Using a variable Δ_{FWHM} instead of this slope we can say that Δ_{FWHM} shows negative values in the lower photosphere. If we put our results together with those of Nesis et al. (1993) we can recognize a reversal of Δ_{FWHM} at heights where $FWHM$ of our line V and the Fe I 6498.945 Å line of Nesis et al. (1993) are formed.

Further results can be seen in Fig. 2: the behaviour of the mean $FWHM$ is different for granular and intergranular data, magnetic and non-magnetic lines, and for higher-formed and lower-formed lines. We find in particular: (1) The variation is not symmetric for the granular and the intergranular case, except for the line I where the point of symmetry has coordinates $x = I_{mean}$ and y = total mean $FWHM$. (2) A conspicuous minimum of the mean $FWHM$ occurs for the intergranular case in magnetic lines at continuum limits of about 0.975. No significant minimum is found in the non-magnetic lines I and IV. We conclude that near the centre of intergranular lanes the photospheric layers are affected by both nonthermal and magnetic processes. Nesis et al. (1991) arrived at a similar conclusion for the lower part of the photosphere. (3) A local maximum of the mean $FWHM$ appears at a continuum limit of about 1.02 for a granular case in both magnetic and non-magnetic lines formed in the lower photosphere. The excess of the mean $FWHM$ in the granular case near the centre of a granulum can be connected to convection because lines III, IV and V are formed in the lower photosphere. (4) A higher relative scattering of the mean $FWHM$ values appears at the deepest level, line V.

© European Southern Observatory • Provided by the NASA Astrophysics Data System

1995A&A...298..917K

Table 3. Mean $FWHM$ values (in mÅ) in granular and intergranular spaces.

Line	Total mean $FWHM$	Threshold 4%			Floating threshold		
		Granulum	Intergranulum	Δ_{FWHM} *)	Granulum	Intergranulum	Δ_{FWHM} *)
I	177.1 ±6.2	173.7 ±5.0	181.3 ±4.4	7.6 = 4.3% +)	171.4 ±0.9	183.4 ±3.6	12.0 = 6.8% +)
II	187.5 ±4.7	183.4 ±3.3	190.0 ±3.6	6.6 = 3.5%	183.4 ±3.3	190.7 ±3.8	7.3 = 3.9%
III	151.1 ±3.2	148.3 ±2.4	152.8 ±1.8	4.5 = 3.0%	148.7 ±2.4	153.3 ±1.7	4.6 = 3.0%
IV	138.5 ±2.5	137.3 ±2.5	140.9 ±2.1	3.6 = 2.6%	137.1 ±2.5	140.7 ±2.1	3.6 = 2.6%
V	121.3 ±4.3	120.6 ±3.8	121.4 ±3.8	0.8 = 0.7%	120.7 ±3.9	122.1 ±3.8	1.4 = 1.2%

*) $\Delta_{FWHM} = (FWHM_{intergranulum} - FWHM_{granulum})$
+) Percent of total mean $FWHM$, as listed in column (2)

3.4. Correlations between line parameters

The correlation coefficients between the investigated line characteristics I_c, I_o, and $FWHM$ are given in Table 4 separately for the NARs, PQRs and MARs. It is evident that these correlations depend on the degree of activity in the observed region (NAR, PQR, or MAR), on the magnetic sensitivity of the line, and on the height of line formation in the atmosphere.

(1) Correlation $< I_c, I_o >$ (Fig. 3): We find an *anticorrelation*. This anticorrelation is more pronounced for the lines III, IV and V which are formed deeper in the photosphere than for lines I and II. The difference between the correlation coefficients calculated for lines I, II and for lines III, IV, V is largest in the PQRs (squares). The maximum of the anticorrelation appears (Fig. 3) at heights of 250 – 350 km; this result is supported by the observations of Balthasar et al. (1990) as well as by those of Komm et al. (1990). At heights of about 500 km the anticorrelation decreases again to lower values. This behaviour can hardly be explained by random coincidence. In spite of a slight uncertainty in the height definition by the different authors, the observed anticorrelation indicates the appearance of structural changes at about 250 – 350 km.

(2) Correlation $< I_c, FWHM >$: The values calculated for the magnetic lines II, III and V differ from the values obtained from the non-magnetic lines. There is a higher anticorrelation for non-magnetic lines, and a higher anticorrelation for all lines in the MARs, as compared to the PQRs. The correlation $< I_c, FWHM >$ for the deepest line (line V) is in agreement with the result of Hanslmeier et al. (1994).

(3) Correlation $< I_o, FWHM >$: For all lines this correlation is higher in the MARs than in the PQRs. There is no difference for magnetic and non-magnetic lines in the PQRs, in contrast to the MARs, where the correlation coefficients for the magnetic lines reach higher values.

Table 4. Averaged correlation coefficients between the spectral parameters for NAR, PQR and MAR.

	NAR		
Line	$< I_c, I_o >$	$< I_c, FWHM >$	$< I_o, FWHM >$
I	-0.30	-0.33	0.60
II	-0.25	-0.15	0.74
III	-0.43	-0.21	0.74
IV	-0.42	-0.34	0.68
V	-0.35	-0.19	0.78
	PQR		
Line	$< I_c, I_o >$	$< I_c, FWHM >$	$< I_o, FWHM >$
I	-0.19	-0.29	0.58
II	-0.21	-0.14	0.65
III	-0.53	-0.21	0.40
IV	-0.47	-0.29	0.47
V	-0.45	-0.15	0.57
	MAR		
Line	$< I_c, I_o >$	$< I_c, FWHM >$	$< I_o, FWHM >$
I	-0.32	-0.41	0.64
II	-0.34	-0.26	0.78
III	-0.46	-0.36	0.85
IV	-0.46	-0.43	0.74
V	-0.41	-0.29	0.81

4. Conclusions

The results presented in this paper for the PQRs and MARs (Figs. 1 and 3) should be discussed together with the earlier observations. The correlation results show that the structure coupled to the granulation continuously weakens with height in the photosphere and disappears at a height of about 200 km. A new structure, similar to the granulation pattern, appears at a height of about 300 km but disappears again at about 500 km. At the same time the residual line-intensity fluctuations, representing mainly temperature fluctuations, reach a minimum at 300 km, just where the new structure appears. These fluctuations increase again at heights around 500 km where no granulation-like structure was detected.

These facts support the existence of the non-convective structure mentioned by Komm et al. (1990, their Fig. 7). For the PQRs and MARs the present work contributes informa-

© European Southern Observatory • Provided by the NASA Astrophysics Data System

1995A&A...298..917K

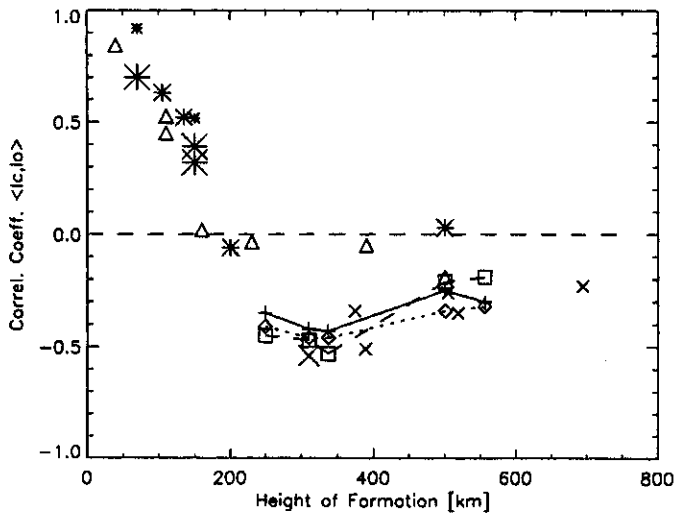

Fig. 3. Correlation coefficient $< I_c, I_o >$, as a function of the height of line formation: △ - Canfield & Mehltretter (1973); big ∗ - Hanslmeier et al. (1993); ∗ - Hanslmeier et al. (1990); small ∗ - Hanslmeier et al. (1994); small × - Balthasar et al. (1990); big × - Komm et al. (1990). The symbols +, ◇ and □ stand for our NAR, MAR and PQR, respectively

tion about that structure, mostly with respect to the height-dependence of its temperature fluctuations.

The new method used for investigation of nonthermal motions shows the local decrease of $FWHM$ for all heights caused by magnetic field near the centres of intergranular lanes. For the granular case the local increase of $FWHM$ for deeper layers indicates the influence of the convective motions near the centres of granules.

For a detailed physical explanation of these observed facts we probably need more numerical simulations of the flows in and above granules and intergranular lanes. In order to increase the statistical weight of our results a larger number of observations, within supergranules and near their boundaries, should be evaluated.

Acknowledgements. We thank H. Schleicher for helpful discussions and for his work on the KIS LIB routines. We are grateful to H. Balthasar, A. Nesis and M. Stix for useful discussions and to the referee, F. Kneer, for his critical comments. JR and AK have been supported by the Slovak Academy of Sciences under grant GA 506/1993. The Vacuum Tower Telescope is operated by the Kiepenheuer-Institut für Sonnenphysik, Freiburg, at the Observatorio del Teide of the Instituto de Astrofísica de Canarias.

References

Balthasar, H., Grosser, H., Schröter, C., & Wiehr, E., 1990, A&A 235, 437
Bruls, J.H.M.J., Lites, B.W. & Murphy, G.A., 1991, in: Solar Polarimetry, ed. L.J. November, National Solar Observatory, Sacramento Peak, Sunspot, p. 444
Canfield, R.C., & Mehltretter, J.P., 1973, Solar Phys. 33, 33
Delbouille, L., Roland, G., & Neven, L., 1973, The Photometric Atlas of the Solar Spectrum, Spec. Volume ed. Institut D'Astrophysique de L'Université de Liege.
Dravins, D., 1982, ARA&A 20, 61
Durrant,C.J., & Nesis, A., 1981, A&A 95, 221
Guenther, E., & Mattig, W., 1991, A&A 243, 244
Hanslmeier, A., Mattig, W., & Nesis, A., 1990, A&A 238, 345
Hanslmeier, A., Mattig, W., & Nesis, A., 1991, A&A 244, 521
Hanslmeier, A., Nesis, A., & Mattig, W., 1993, A&A 270, 516
Hanslmeier, A., Nesis, A., & Mattig, W., 1994, A&A 288, 960
Holweger, H., & Kneer, F., 1989, in: Solar and Stellar Granulation, eds. R.J. Rutten, G. Severino, Kluwer, London, p. 173
Keil, S.L., & Canfield, R.C., 1978, A&A 70, 169
Kneer, F., Mattig, W., Nesis, A., & Werner, W., 1980, Solar Phys. 68, 31
Komm, R., Mattig, W., & Nesis, A., 1990, A&A 239, 340
Lites, B.V., Nordlund, Å., Scharmer, G.B., 1989, in: Solar and Stellar Granulation, eds. R.J. Rutten, G. Severino, Kluwer, London, p. 349
Muller, R., 1985, Solar Phys. 100, 237
Muller, R., 1989, in: Solar and Stellar Granulation, eds. R.J. Rutten, G. Severino, Kluwer, London, p. 101
Nesis, A., Hanslmeier, A., Hammer, R., Komm, R., & Mattig, W., 1991, in: Mechanisms of Chromospheric and Coronal Heating, eds. P. Ulmschneider, E.R. Priest, R. Rosner, Springer, Heidelberg, p.36
Nesis, A., Hanslmeier, A., Hammer, R., Komm, R., Mattig, W., & Staiger, J., 1992a, A&A 253, 561
Nesis, A., Hanslmeier, A., Hammer, R., Komm, R., Mattig, W., & Staiger, J., 1992b, in: Cool Stars, Stellar Systems and the Sun, eds. M. Giampapa and J.A. Bookbinder, Tucson, Arizona, PASPC, Vol. 26, p.181
Nesis, A., Bogdan, T.J., Cattaneo, F., Hanslmeier, A., Knölker, M., & Malagoli, A., 1992c, Ap.J. 399, L99
Nesis, A., Hanslmeier, A., Hammer, R., Komm, R., Mattig, W., & Staiger, J., 1993, A&A 279, 599
Schröter, E.H., Soltau, D., & Wiehr, E., 1985, Vistas in Astronomy, Vol. 28, 519
Soltau, D., 1989, in: High Spatial Resolution Solar Observations, ed. O. von der Lühe, National Solar Observatory, Sacramento Peak, Sunspot, p. 3
Spruit, H.C., Nordlund, Å ., & Title A.M. 1990, ARA&A 28, 263
Wiehr, E., & Kneer F., 1988, A&A 195, 310

This article was processed by the author using Springer-Verlag TEX A&A macro package 1992.

© European Southern Observatory • Provided by the NASA Astrophysics Data System